frontiers in Materials

ORIGINAL RESEARCH
published: 13 August 2018
doi: 10.3389/fmats.2018.00041

Mechanical Properties of Nanostructured CoCrFeNiMn High-Entropy Alloy (HEA) Coating

Chaoqun Dang[1,2], *James U. Surjadi*[2], *Libo Gao*[1,2] *and Yang Lu*[1,2]*

[1] Centre for Advanced Structural Materials, Shenzhen Research Institute, City University of Hong Kong, Shenzhen, China,
[2] Department of Mechanical and Biomedical Engineering, City University of Hong Kong, Kowloon, Hong Kong

An equiatomic CoCrFeMnNi high-entropy alloy (HEA) thin film coating has been successfully developed by high-vacuum Radio Frequency (RF) magnetron sputtering. The deposition of a smooth and homogenous thin film with uniformly distributed equiaxed nanograins (grain size ~ 10 nm) was achieved through this technique. The thin film coating exhibits a high hardness of 6.8 ± 0.6 GPa, which is superior compared to its bulk counterpart owing to its nanocrystalline structure. Furthermore, it also shows good ductility through nanoindentation, which demonstrates its potential to serve as an alternative to traditional transition metal nitride or carbide coatings for applications in micro-fabrication and advanced coating technologies.

Keywords: high-entropy alloy (HEA), thin film coating, nanograined structure, nanoindentation, hardness

OPEN ACCESS

Edited by:
Sheng Guo,
Chalmers University of Technology, Sweden

Reviewed by:
Amir Motallebzadeh,
Koç University, Turkey
Zhiyuan Liu,
Shenzhen University, China

****Correspondence:***
Yang Lu
yanglu@cityu.edu.hk

Specialty section:
This article was submitted to Structural Materials, a section of the journal Frontiers in Materials

Received: *23 March 2018*
Accepted: *14 June 2018*
Published: *13 August 2018*

Citation:
Dang C, Surjadi JU, Gao L and Lu Y (2018) Mechanical Properties of Nanostructured CoCrFeNiMn High-Entropy Alloy (HEA) Coating. Front. Mater. 5:41. doi: 10.3389/fmats.2018.00041

INTRODUCTION

In the past decades, binary (Ye Y. et al., 2015a; Li et al., 2018), ternary (Yao et al., 2015; Ye Y. et al., 2015b) and quaternary (Dang et al., 2017; Wang et al., 2017) transition metal nitride or carbide coatings have been well explored and applied in many industrial and engineering fields. These coatings possess very high hardness, but their brittle property has impeded its application in certain areas, such as automotive parts, mold, tools etc. In recent years, compositionally complex alloys consisting of five or more principal elements, frequently referred to as high-entropy alloys (HEAs) have emerged and attracted increasing attention (Cantor et al., 2004; Yeh et al., 2004; Zhang et al., 2013; Ye Y. F. et al., 2015a,b; Tian, 2017; Jin and Bei, 2018) due to their unique compositions, multi-component solid-solution structures, excellent mechanical behaviors and potential industrial applications. HEAs with multi-element solid-solution exhibits a large solid solubility which allows HEAs to have a combination of high strength, excellent oxidation resistance, high wear resistance, and corrosion resistance, making them an ideal candidate for high performance coating applications.

As HEAs are solid-solution alloys consisting of five or more elements in equiatomic proportions, it can have numerous possible combinations. For instance, solid-solution hardening (high strength) with good ductility can be achieved when the solid-solution phase exhibits a simple crystal structure (Otto et al., 2013), e.g., face-centered cubic (FCC), with many slip systems. Structural materials require both high strength and ductility, properties that are often mutually exclusive. Therefore, research efforts have tended to be application driven and directed toward exploring new alloy compositions with promising mechanical properties (Otto et al., 2013). By combining the excellent mechanical performance of HEAs with thin film technology, HEA coatings have been shown to exhibit properties that significantly surpass its bulk counterpart, further increasing its application potential (Yan et al., 2017). Gao et al. have found that $CoCrFeNiAl_{0.3}$ metallic film has a nanocrystalline structure (grain size ~10 nm) and its hardness is about four times of that of the

bulk single-crystal counterpart (Gao et al., 2017; Liao et al., 2017). Damage tolerance of the high-entropy alloy CrMnFeCoNi (Zhang et al., 2015) was studied and the authors found that the single-phase CrMnFeCoNi alloy displays tensile strength levels of ∼1 GPa, excellent ductility (∼60–70%) and exceptional fracture toughness ($K_{JIc} > 4{,}200$ MPa $m^{1/2}$). Herein, we propose a CrMnFeCoNi alloy thin film and study whether it can possess a high hardness and ductility as the bulk ones.

In the present work, an equiatomic CoCrFeMnNi high-entropy thin film coating was developed and deposited by high-vacuum RF magnetron sputtering. The microstructures of the film were systematically studied by scanning electron microscopy (SEM) and transmission electron microscopy (TEM). Its mechanical properties were carefully characterized by nanoindentation and Vickers indentation. Cross-sectional Focused Ion Beam (FIB) images of the Vickers indentation were used to investigate the ductility and crack propagation of the CoCrFeMnNi high-entropy thin film.

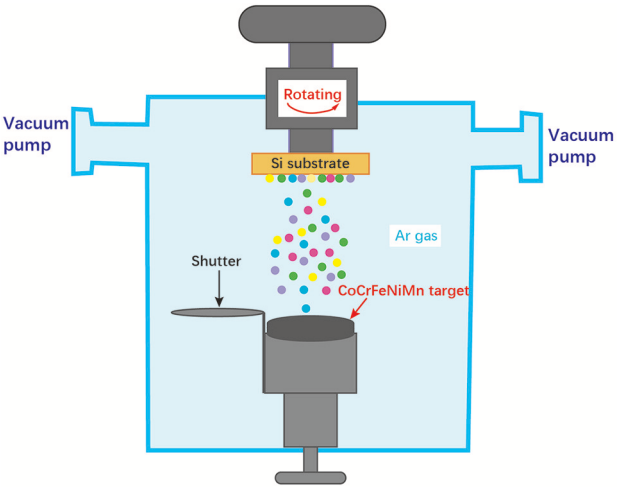

FIGURE 1 | Schematic illustration of the CoCrFeNiMn high-entropy thin film fabrication method.

METHODS

CoCrFeNiMn high-entropy thin films were deposited on silicon substrates by high-vacuum RF magnetron sputtering, shown in **Figure 1**. We selected the $Co_{20}Cr_{20}Fe_{20}Ni_{20}Mn_{20}$ (at%) alloy as the target that was synthesized by vacuum melting with high purity (>99.99%) raw materials of cobalt, chromium, iron, nickel, and manganese. Before deposition, the silicon substrates were ultrasonically cleaned for 15 min, followed with acetone, ethanol and deionized water, respectively. The substrate was mounted on a pre-cleaned substrate holder and fixed on the carousel in the deposition chamber with a working distance of about 80 mm. The rotation speed of the substrate holder was set as 2 rpm to guarantee a homogeneous deposition. The background pressure was pumped to 1.0×10^{-6} Pa, and then high purity argon was introduced into the vacuum chamber. The ignition argon flow was set to be 22 standard cubic centimeters per minute (sccm), while the subsequent stable argon flow of argon flow rate was fixed at 12 sccm. The sputtering was conducted at room temperature, with the deposition time set for 30 min at 350 W power.

Surface and cross-section morphologies of the CoCrFeNiMn HEA thin film were characterized by a field-emission scanning electron microscope (SEM, Quanta 450, FEI, Hillsboro, OR, USA) equipped with an energy dispersive X-ray spectrometer (EDX, Oxford Instruments, Oxford, UK) operated at 10 kV. Chemical composition of the film was measured by EDS. X-ray diffraction (XRD) patterns were recorded on a Bruker D8 Advance X-ray diffractometer running in the BraggBrentano geometry using Cu Kα radiation ($\lambda = 0.154$ nm). TEM analysis (bright-field imaging and selected area electron diffraction) for the CoCrFeNiMn high-entropy alloy thin film was conducted with a field-emission transmission electron microscope (JEOL, model JEM-2100F FE-TEM). The measurements of elastic modulus (E) and hardness (H) were performed by the load-depth-sensing nanoindentation equipped with a Berkovich triangular pyramid indenter. The maximum indentation depth was set as 100 nm. The hardness and elastic modulus were calculated according to the Oliver-Pharr method from the load displacement curves as an average from 49 indents. Hardness map was determined, where the indents were 5 μm from each other in a 30 × 30 μm array. To evaluate the toughness of the CoCrFeNiMn high-entropy alloy thin film, a nanoindenter with a maximum applied load of 500 mN was adopted. The surface and cross-sectional morphologies of the indentations were then examined by SEM and focused ion beam (FIB) to evaluate the cracks and degree of coating delamination around the indentations.

RESULTS AND DISCUSSION

Figure 2 shows cross-sectional, plan-view SEM images and SEM-EDS mapping of the CoCrFeNiMn high-entropy thin film. A smooth and homogenous cross-section could be observed in **Figure 2a**, with an average film thickness of ∼300 nm. From the plan-view morphology, the film has a smooth surface and without any defects. **Figure 2c** shows a uniform distribution of the five elements, with no other elements found among the film surface. In addition, chemical composition of the Co, Cr, Fe, Ni and Mn is 19.3 at.%, 19.9 at.%, 19.1 at.%, 19.1 at.% and 22.6 at.%, of which the atomic ratio of Co: Cr: Fe: Ni: Mn the is very close to 1:1:1:1:1, and it is nearly identical with its bulk counterpart.

The microstructural characterization is performed using XRD and TEM. **Figure 3** shows XRD pattern obtained from the CoCrFeNiMn high-entropy thin film. It can be clearly observed that the CoCrFeNiMn high-entropy thin film is composed of both simple FCC and BCC solid solution phase. **Figure 4** shows representative TEM, HR-TEM, inverse FFT images obtained using spots indicated in **Figure 4b** and the corresponding Selected Area Electron Diffraction (SAED) pattern of the CoCrFeNiMn high-entropy alloy thin film. As shown in **Figures 4a,b** the film contains homogeneously

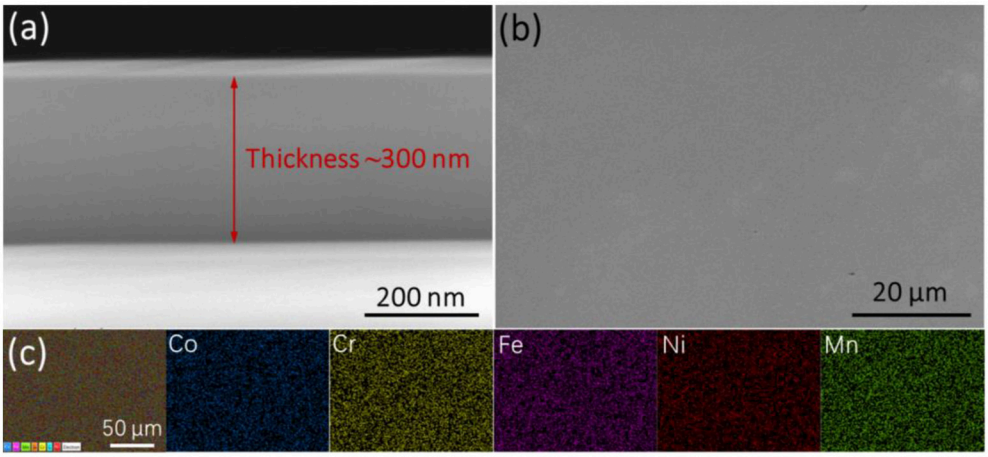

FIGURE 2 | Cross-sectional **(a)**, plan-view **(b)** SEM images, and SEM-EDS mapping **(c)** images of the CoCrFeNiMn high-entropy thin film, indicating the homogeneous element distribution.

distributed equiaxed nanograins with an average grain size of ~10 nm. Generally, nanograined metals possess high strength and hardness due to the formation of nanocrystalline grains, which is beneficial for the mechanical enhancement of the HEA film (Lu et al., 2009; Fang et al., 2011). The space of the lattice fringe marked in **Figure 4b** was calculated to be 2.20 Å, which corresponds to the spacing of the FCC HEA (200) planes. The SAED pattern from the overall structure also strongly implies that the film possesses a polycrystalline nanostructure. Diffraction pattern shows strong rings correlated with FCC phases and very weak reflections ascribed with BCC phases. The calculated values of the lattice parameters agree well with that of another research (Schuh et al., 2015), in which the film mainly consists of FCC phases and a small fraction of BCC phases.

Figure 5 shows the hardness, elastic modulus (**Figure 5a**) and hardness map (**Figure 5b**) of the CoCrFeNiMn high-entropy alloy thin film. The average hardness and elastic modulus were calculated according to the Oliver-Pharr method from the load-displacement curves as an average from 49 indents. An average of 49 indents on the film results in an elastic modulus of 176.8 ± 2.4 GPa and a hardness of 6.8 ± 0.6 GPa, of which the hardness is much higher than its bulk counterpart (Lee et al., 2016; Maier-Kiener et al., 2017) as shown in **Figure 5a**. The increase of hardness may due to nanograined microstructure and Physical Vapor Deposition (PVD) technique, since melting bulk HEA materials of traditional approach exhibit very large grain sizes in the micrometer-scale. To study the hardness distribution of the film, hardness maps were determined, where the indents were 5 µm from each other in a 30 × 30 µm array. The film exhibits a variation in hardness, as shown by the hardness map in **Figure 5b**. As other research reported, the single-phase BCC HEAs usually have very high strength and low ductility while single-phase FCC HEAs typically exhibit low strength and high ductility (Liao and Baker, 2011; Praveen et al., 2012; Pradeep et al., 2013; Senkov et al., 2014; Schuh et al., 2015; Song et al., 2018). Therefore, if the indent is over an area where the FCC phase concentration is high, low hardness down to 5.8 GPa could be obtained owing to the low hardness of the FCC phase. On the other hand, when the indent is over an area where the concentration of BCC phase is high, hardness up to 7.8 GPa was obtained, because BCC phase has a relatively high hardness.

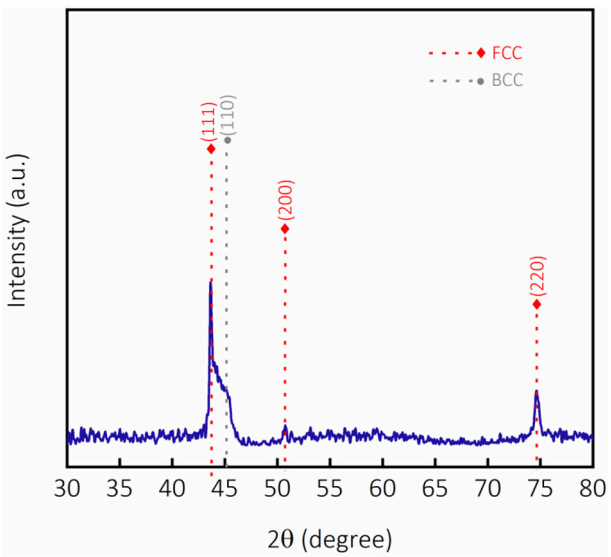

FIGURE 3 | XRD pattern obtained from the CoCrFeNiMn high-entropy thin film.

Despite the superior hardness of the HEA film, it is also crucial to assess its ductility. Herein, we performed nanoindentation a maximum indentation load of 500 mN to qualitatively evaluate the ductility of the CoCrFeNiMn high-entropy alloy thin film. Subsequently, the surface and cross-sectional morphology of the indentations were examined by SEM and FIB to evaluate the cracks and degree of film delamination around the indentations.

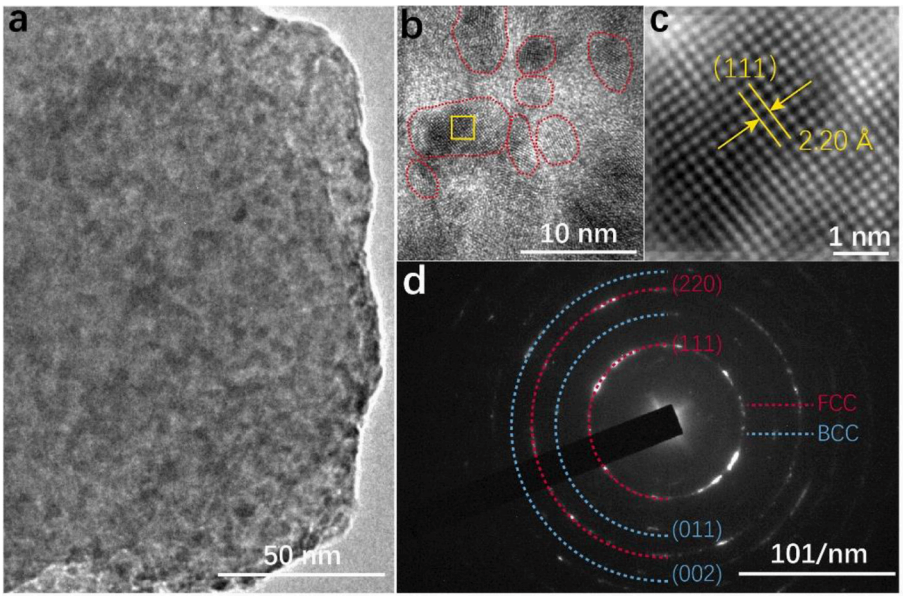

FIGURE 4 | Representative TEM **(a)**, HR-TEM **(b)**, inverse FFT **(c)** obtained using spots indicated by the rectangle region in **(b)** and corresponding SAED pattern **(d)** of the CoCrFeNiMn high-entropy thin film, suggesting its polycrystalline structures.

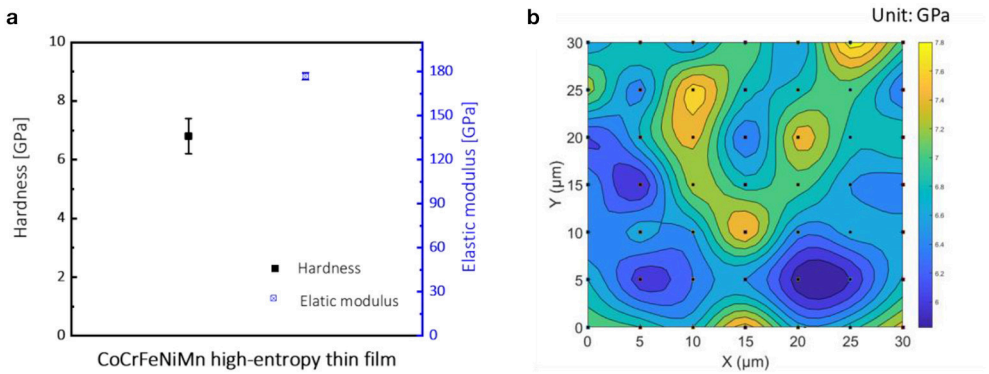

FIGURE 5 | Hardness, elastic modulus **(a)**, and hardness mapping **(b)** of the CoCrFeNiMn high-entropy thin film.

Figures 6a,b shows plan-view SEM images of nanoindentation induced cracking at an applied load of 500 mN. Plastic deformation, represented by the stacked layers of HEA film at the indentation edge can be found, as shown in the plan-view and tilted SEM images (**Figures 6b,c**). Cross-section in **Figure 6c** of the deformed indentation was milled by FIB and is shown in **Figure 6d**. A large crack (indicated by arrows) along the radial direction of the indentation was formed, which induces the crack initiation and propagation in the film. In addition, a crack initiating from the middle cross-section of the film (**Figure 6d**) could also be found, as indicated by the arrows. Plastic deformation and stacking can be clearly found in **Figure 6d** as well. According to the above analyses, the CoCrFeNiMn high-entropy thin film not only possess a high hardness but also exhibits a good ductility. In addition to its excellent hardness and ductility in comparison to transition metal nitride or carbide coatings, the novel alloy design of HEAs allows it to possess unique properties to cater for specialized applications, signifying its immense potential for industrial applications.

CONCLUSION

In summary, it is found that magnetron sputtering can be an efficient and effective technique to deposit high-quality equiatomic HEA thin films with smooth and homogeneous microstructure. The film has a thickness of ∼300 nm, and mainly possesses FCC crystalline phases and with a small a fraction of BCC phases. The elastic modulus of the film is 176.8 ± 2.4 GPa and the hardness is 6.8 ± 0.6 GPa, of which the hardness is much higher than its bulk counterpart due to the

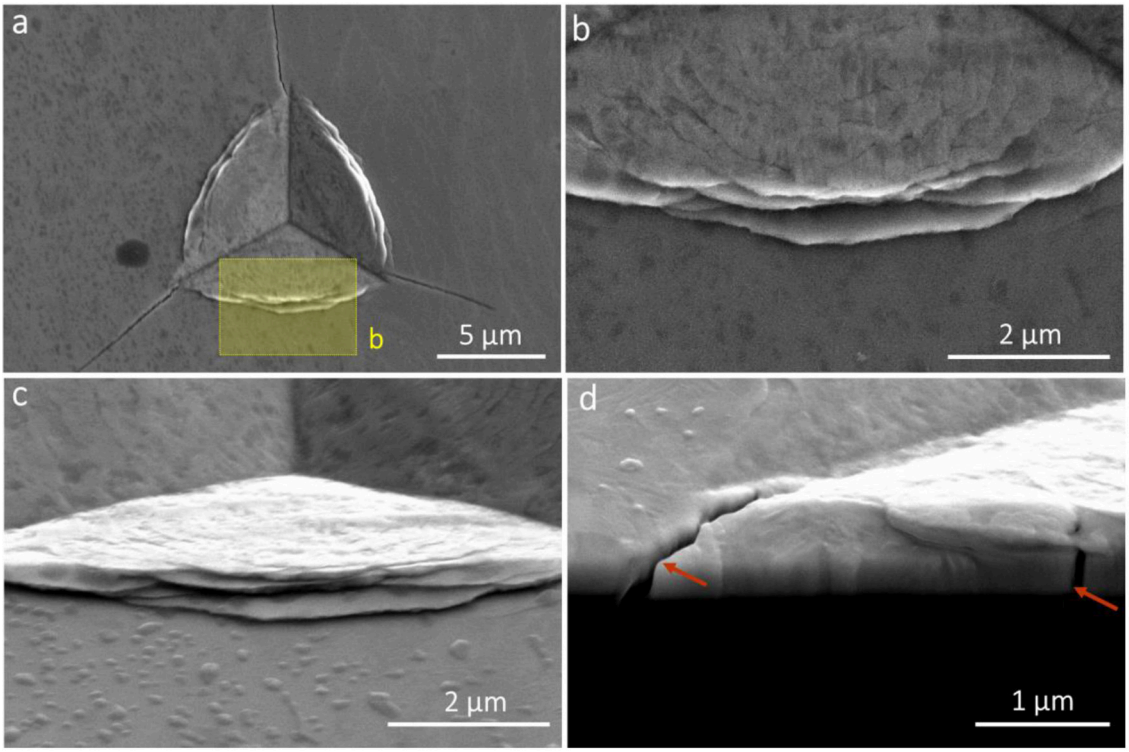

FIGURE 6 | SEM images of nanoindentation induced cracking at an applied load of 500 mN. Representative SEM images: plan-view **(a)**, close-up view of stacked layers **(b)**, indentation at 52° tilt **(c)**, and cross-sectional SEM image **(d)** milled by FIB for the nanoindentation induced cracking at a penetration load of 500 mN.

formation of a nanocrystalline structure. Furthermore, the film also shows a good ductility through nanoindentation testing, which indicates that it could be a promising substitute to traditional transition metal nitride or carbide coatings for some specialized applications in the micro-fabrication and advanced coating industries.

AUTHOR CONTRIBUTIONS

CD designed and fabricated samples, conducted experiments, analyzed data, and wrote the manuscript. JS and LG performed the TEM experiments, analyzed data, and wrote manuscript partially. YL supervised the research and revised the manuscript. All the authors participated in discussions of the research and have given approval to the final version of the paper.

ACKNOWLEDGMENTS

The authors gratefully thank the funding support from Shenzhen Science and Technology Innovation Committee under the grants JCYJ20160401100358589. The authors also thank the funding support from City University of Hong Kong (Project 9680108).

REFERENCES

Cantor, B., Chang, I. T. H., Knight, P., and Vincent, A. J. B. (2004). Microstructural development in equiatomic multicomponent alloys. *Mater. Sci. Eng. A* 375–377, 213–218. doi: 10.1016/j.msea.2003.10.257

Dang, C., Li, J., Wang, Y., Yang, Y., Wang, Y., and Chen, J. (2017). Influence of Ag contents on structure and tribological properties of TiSiN-Ag nanocomposite coatings on Ti−6Al−4V. *Appl. Surf. Sci.* 394, 613–624. doi: 10.1016/j.apsusc.2016.10.126

Fang, T. H., Li, W. L., Tao, N. R., and Lu, K. (2011). Revealing extraordinary intrinsic tensile plasticity in gradient nano-grained copper. *Science* 331, 1587–1590. doi: 10.1126/science.1200177

Gao, L., Liao, W., Zhang, H., Surjadi, J., Sun, D., and Lu, Y. (2017). Microstructure, mechanical and corrosion behaviors of CoCrFeNiAl0.3 high entropy alloy (HEA) films. *Coatings* 7:156. doi: 10.3390/coatings7100156

Jin, K., and Bei, H. (2018). Single-phase concentrated solid-solution alloys: bridging intrinsic transport properties and irradiation resistance. *Front. Mater.* 5:26. doi: 10.3389/fmats.2018.00026

Lee, D. H., Seok, M. Y., Zhao, Y., Choi, I. C., He, J., Lu, Z., et al. (2016). Spherical nanoindentation creep behavior of nanocrystalline and coarse-grained CoCrFeMnNi high-entropy alloys. *Acta Mater.* 109, 314–322. doi: 10.1016/j.actamat.2016.02.049

Li, Z., Wang, Y., Cheng, X., Zeng, Z., Li, J., Lu, X., et al. (2018). Continuously growing ultra-thick CrN coating to achieve high load bearing capacity and good tribological property. *ACS Appl. Mater. Interfaces* 10, 2965–2975. doi: 10.1021/acsami.7b16426

Liao, W., Lan, S., Gao, L., Zhang, H., Xu, S., Song, J., et al. (2017). Nanocrystalline high-entropy alloy ($CoCrFeNiAl_{0.3}$) thin-film coating by magnetron sputtering. *Thin Solid Films* 638, 383–388. doi: 10.1016/j.tsf.2017.08.006

Liao, Y., and Baker, I. (2011). On the room-temperature deformation mechanisms of lamellar-structured $Fe_{30}Ni_{20}Mn_{35}Al_{15}$. *Mater. Sci. Eng. A* 528, 3998–4008. doi: 10.1016/j.msea.2011.01.089

Lu, K., Lu, L., and Suresh, S. (2009). Strengthening materials by engineering coherent internal boundaries at the nanoscale. *Science* 324, 349–352. doi: 10.1126/science.1159610

Maier-Kiener, V., Schuh, B., George, E. P., Clemens, H., and Hohenwarter, A. (2017). Nanoindentation testing as a powerful screening tool for assessing phase stability of nanocrystalline high-entropy alloys. *Mater. Design* 115, 479–485. doi: 10.1016/j.matdes.2016.11.055

Otto, F., Dlouhý, A., Somsen, C., Bei, H., Eggeler, G., and George, E. P. (2013). The influences of temperature and microstructure on the tensile properties of a CoCrFeMnNi high-entropy alloy. *Acta Mater.* 61, 5743–5755. doi: 10.1016/j.actamat.2013.06.018

Pradeep, K. G., Wanderka, N., Choi, P., Banhart, J., Murty, B. S., and Raabe, D. (2013). Atomic-scale compositional characterization of a nanocrystalline AlCrCuFeNiZn high-entropy alloy using atom probe tomography. *Acta Mater.* 61, 4696–4706. doi: 10.1016/j.actamat.2013.04.059

Praveen, S., Murty, B. S., and Kottada, R. S. (2012). Alloying behavior in multi-component AlCoCrCuFe and NiCoCrCuFe high entropy alloys. *Mater. Sci. Eng. A* 534, 83–89. doi: 10.1016/j.msea.2011.11.044

Schuh, B., Mendez-Martin, F., Völker, B., George, E. P., Clemens, H., Pippan, R., et al. (2015). Mechanical properties, microstructure and thermal stability of a nanocrystalline CoCrFeMnNi high-entropy alloy after severe plastic deformation. *Acta Mater.* 96, 258–268. doi: 10.1016/j.actamat.2015.06.025

Senkov, O. N., Senkova, S. V., and Woodward, C. (2014). Effect of aluminum on the microstructure and properties of two refractory high-entropy alloys. *Acta Mater.* 68, 214–228. doi: 10.1016/j.actamat.2014.01.029

Song, R., Wei, L., Yang, C., and Wu, S. (2018). Phase formation and strengthening mechanisms in a dual-phase nanocrystalline CrMnFeVTi high-entropy alloy with ultrahigh hardness. *J. Alloys Compd.* 744, 552–560. doi: 10.1016/j.jallcom.2018.02.029

Tian, F. (2017). A review of solid-solution models of high-entropy alloys based on *ab initio* calculations. *Front. Mater.* 4:36. doi: 10.3389/fmats.2017.00036

Wang, Y., Li, J., Dang, C., Wang, Y., and Zhu, Y. (2017). Influence of carbon contents on the structure and tribocorrosion properties of TiSiCN coatings on Ti6Al4V. *Tribol. Int.* 109, 285–296. doi: 10.1016/j.triboint.2017.01.002

Yan, X. H., Li, J. S., Zhang, W. R., and Zhang, Y. (2017). A brief review of high-entropy films. *Mater. Chem. Phys.* 210, 12–19. doi: 10.1016/j.matchemphys.2017.07.078

Yao, Y., Li, J., Wang, Y., Ye, Y., and Zhu, L. (2015). Influence of the negative bias in ion plating on the microstructural and tribological performances of Ti-Si-N coatings in seawater. *Surf. Coat. Technol.* 280, 154–162. doi: 10.1016/j.surfcoat.2015.09.005

Ye, Y., Wang, Y., Chen, H., Li, J., Yao, Y., and Wang, C. (2015a). Doping carbon to improve the tribological performance of CrN Coatings in seawater. *Tribol. Int.* 90, 362–371. doi: 10.1016/j.triboint.2015.04.008

Ye, Y., Wang, Y., Wang, C., Li, J., and Yao, Y. (2015b). An analysis on tribological performance of CrCN coatings with different carbon contents in seawater. *Tribol. Int.* 91, 131–139. doi: 10.1016/j.triboint.2015.07.002

Ye, Y. F., Liu, C. T., and Yang, Y. (2015a). A geometric model for intrinsic residual strain and phase stability in high entropy alloys. *Acta Mater.* 94, 152–161. doi: 10.1016/j.actamat.2015.04.051

Ye, Y. F., Wang, Q., Lu, J., Liu, C. T., and Yang, Y. (2015b). Design of high entropy alloys: a single-parameter thermodynamic rule. *Scr. Mater.* 104, 53–55. doi: 10.1016/j.scriptamat.2015.03.023

Yeh, J., Chen, S., Gan, J., Lin, S., and Chin, T. (2004). Communications: formation of simple crystal structures in Cu-Co-Ni-Cr-Al-Fe-Ti-V alloys with multiprincipal metallic elements. *Metall. Mater. Trans.* 35, 2533–2536. doi: 10.1007/s11661-006-0234-4

Zhang, Y., Zuo, T. T., Tang, Z., Gao, M. C., Dahmen, K. A., Liaw, P. K., et al. (2013). Microstructures and properties of high-entropy alloys. *Prog. Mater. Sci.* 61, 1–93. doi: 10.1016/j.pmatsci.2013.10.001

Zhang, Z. J., Mao, M. M., Wang, J., Bernd, G., Zhang, Z., Mao, S. X., et al. (2015). Nanoscale origins of the damage tolerance of the high-entropy alloy CrMnFeCoNi. *Nat. Commun.* 6:10143. doi: 10.1038/ncomms10143

Conflict of Interest Statement: The authors declare that the research was conducted in the absence of any commercial or financial relationships that could be construed as a potential conflict of interest.